promote ring opening of I by withdrawing electron density from the P–N bonds. It has been shown repeatedly at 170 °C without BCl_3 present that I remains unchanged over long periods of time while polymerization is facile at this temperature when BCl_3 is present.

The absence of a termination step is indicated by the molecular weight dependence on conversion (Table II) and the ability to start and stop the reaction without affecting k_{obsd}.

Conclusions

BCl_3 has both advantages and limitations as a catalyst for the polymerization of I. Optimum rates of propagation require BCl_3 in excess of [II] throughout the course of the reaction. This excess of catalyst imposes a state of continuous initiation on the system and does not give extremely high molecular weight polymers or polymers with narrow molecular weight distributions. In addition, the kinetic activation parameters favor propagation over initiation as the temperature is increased. This defeats one of the primary objectives of using a catalyst, which is to lower the polymerization temperature.

One advantage of the BCl_3-catalyzed system is that high yields of un-cross-linked polymer are produced consistently. The reason for this benefit is not fully understood, but it may be due to steric factors, as follows. The nitrogen atom of the phosphazene molecule is the most probable site of attack of the cationic chain end and it is apparent from models of the polymer chain and I that the N atoms in I are more accessible than those in the polymer.[20,21] The effect of steric hindrance is more likely to be a factor in the catalyzed polymerization since the size of the ion pair at the chain end (BCl_4^-) is much larger than in the uncatalyzed system (Cl^-).

Research in our laboratories is directed at positive identification of the polymer end groups, identification of the initiation products, and further enhancement of the reactivity of the growing chain end.

Registry No. I, 940-71-6; II (SRU), 26085-02-9; II (homopolymer), 25231-98-5; BCl_3, 10294-34-5; triphenyl phosphate, 115-86-6.

References and Notes

(1) Allcock, H. R. "Phosphorus–Nitrogen Compounds"; Academic Press: New York, 1972; Chapter 15.
(2) Hagnauer, G. L. *J. Macromol. Sci., Chem.* **1981**, *A16* (1), 385.
(3) Konecny, J. O.; Douglas, C. M. *J. Polym. Sci.* **1959**, *36*, 195.
(4) Knoessel, R.; Parrod, J.; Benoit, H. *C. R. Hebd. Seances Acad. Sci.* **1960**, *25*, 2944.
(5) Allcock, H. R.; Best, R. J. *Can. J. Chem.* **1964**, *42*, 447.
(6) Snyder, D. L.; Stayer, M. L.; Kang, J. W. *U.S. Patent* 4 123 503, 1978.
(7) Devadoss, E.; Nair, C. P. R. *Ind. Eng. Chem. Prod. Res. Dev.* **1984**, *23*, 272.
(8) Fieldhouse, J. W.; Fenske, S. L. *U.S. Patent* 4 327 064, 1982.
(9) Sennett, M. S. Ph.D. Thesis, Northeastern University, 1985.
(10) Hagnauer, G. L.; Koulouris, T. N. "Liquid Chromatography of Polymers and Related Materials III"; Cazes, J., Ed.; Marcel Dekker: New York, 1981.
(11) Allcock, H. R.; Gardner, J. E.; Smeltz, K. M. *Macromolecules* **1975**, *8*, 36.
(12) Fieldhouse, J. W.; Graves, D. F. *U.S. Patent* 4 226 840, 1980.
(13) Moran, E. F. *J. Inorg. Nucl. Chem.* **1968**, *30*, 1405.
(14) Horn, H.-G.; Kolkmann, F. *Makromol. Chem.* **1982**, *183*, 1833.
(15) Horn, H.-G.; Kolkmann, F. *Makromol. Chem.* **1982**, *183*, 1843.
(16) Coxon, G. E.; Sowerby, D. B. *J. Chem. Soc. A* **1969**, 3012.
(17) Patat, F.; Frombling, K. *Monatsh. Chem.* **1955**, *86*, 718.
(18) Chakrabartty, D.; Gosh, B. N. *J. Polym. Sci.* **1962**, *62*, 5130.
(19) MacCallum, J. R.; Werninck, A. *J. Polym. Sci., Part A-1* **1967**, *5*, 3061.
(20) Painter, P. C.; Zarian, J.; Coleman, M. M. *Appl. Spectrosc.* **1982**, *36* (3), 265.
(21) Painter, P. C.; Zarian, J.; Coleman, M. M. *Appl. Spectrosc.* **1982**, *36* (3), 277.

Holographic Relaxation Spectroscopy of Human IgG: Photoinduced Aggregation

Ubonwan A. Stewart and Charles S. Johnson, Jr.*

Department of Chemistry, University of North Carolina, Chapel Hill, North Carolina 27514

Don A. Gabriel*

Department of Medicine, University of North Carolina, Chapel Hill, North Carolina 27514.

Received November 18, 1985

ABSTRACT: Holographic relaxation spectroscopy (HRS) was used to study diffusion and photoinduced reactions of human immunoglobulin G (IgG) labeled with 5-isothiocyanatofluorescein (FITC) and *p*-isothiocyanatoazobenzene (ABITC). Excitation with 488-nm pulses was found to induce aggregation of IgG-FITC, which was initially monomeric. The laser-induced gratings could be detected by diffraction because of the different diffusion rates of the monomers and aggregates. The diffusion coefficients, extrapolated to zero concentration, for the fast and slow species were $(4.5 \pm 0.5) \times 10^{-7}$ and $(2.1 \pm 0.1) \times 10^{-7}$ cm^2/s, respectively. Aggregation was inhibited both by the introduction of reducing agents and by the removal of oxygen, suggesting protein cross-linking assisted by singlet oxygen. IgG-ABITC prepared with pH greater than 11 initially consisted of aggregates, and excitation at 488 nm again produced a grating of monomers and aggregates. However, in this case reducing agents and the removal of oxygen had little effect. Photodisaggregation associated with the trans–cis conformational change of ABITC is suggested.

Introduction

Immunoglobulins are a diverse group of proteins which are synthesized by lymphocytes that form part of the human host defense mechanism. The biological function of the immunoglobulins, or antibodies, involves at least in part the interaction of the immunoglobulin with another species, the antigen. The antigen–antibody reaction may occur in solution or on the surface of a cell. In any event the position and orientation of the antibody with respect to the antigen are critical since the Fab portion of the

0024-9297/86/2219-0964$01.50/0

antibody must interact with the antigen. Thus, the rate of diffusion of the antibody in solutions and in biological matrices is of considerable importance.

We have studied the diffusion and photoinduced reactions of human immunoglobulin G (IgG) by means of a laser light scattering technique, holographic relaxation spectroscopy (HRS).[1,2] In this experiment the molecules of interest are tagged with photochromic or photobleachable labels. The sample is then exposed to a laser interference pattern (writing pulse) and the rate of decay (or smearing out) of the resulting grating of photoproducts is measured. We accomplish this by monitoring the intensity of light diffracted from a low-power laser probe beam (reading beam) by the sample. A major advantage of this method is its selectivity; e.g., the movement of labeled molecules can be studied in complex mixtures. Thus this method provides a uniquely powerful means for studying diffusion and mobility of macromolecules in biological matrices such as gels.

An ideal label molecule for proteins in HRS experiments would (1) be easily attached under mild conditions, (2) leave the protein structure/activity unchanged, and 3) give large diffraction signals. Derivatives of azobenzene, in particular *p*-isothiocyanatoazobenzene (ABITC), are sometimes acceptable labels, but the signals tend to be weak and conjugation is difficult with some proteins.[3] The fluorescent label 5-isothiocyanatofluorescein (FITC), which is easily conjugated with proteins, is known to bleach at relatively low laser powers.[4] Fluorescence is unimportant in HRS, but bleaching should lead to changes in the absorption spectrum and therefore to diffraction of a probe beam. In fact the cesium salt of fluorescein has been used as a label in the holographic study of diffusion in molten polystyrene.[5] However, our previous attempts to use FITC as a label for serum albumin have produced no signals, and we have concluded that the absorption spectrum is not significantly modified by exposure to green light in the HRS experiment.

As part of our continuing program to characterize useful photochromic and photobleachable labels, we report an HRS study of human IgG labeled with FITC and with ABITC. Satisfactory signals were obtained in both cases, but for different reasons. To anticipate the results, we have found that IgG labeled with FITC undergoes photoinduced aggregation but has no significant change in its absorption spectrum when exposed to the writing pulse. Thus, diffraction results only from the different rates of decay of the laser-induced gratings of monomers and aggregates; i.e., the monomer pattern smears out first, leaving a grating of aggregates. In contrast to this, IgG labeled with ABITC under severe conditions consists of a mixture of aggregates prior to exposure to the writing pattern. Excitation of IgG-ABITC by the writing beams produces both a change in the absorption spectrum and a change in the degree of aggregation. In both experiments we were able to measure diffusion coefficients for monomers and aggregates.

Experimental Section

A. Materials. Highly purified IgG was obtained from Sandoz Ltd. The labeling compounds FITC and ABITC were purchased from Trans World Co. and Sigma Chemical Co., respectively. Glutathione and *d*-penicillamine were purchased from Sigma Chemical Co. and were used without further purification.

B. Sample Preparation. The reaction of IgG with FITC was carried out at room temperature for 2 h in 0.1 M NaCl, 0.05 M Tris buffer at pH 8.0, and the reaction of IgG with ABITC was carried out overnight at 4 °C in 0.1 M NaCl, 0.05 M $NaHCO_3$ at pH 11.7. The resulting solutions were dialyzed against 0.1 M NaCl, 0.05 M Tris at pH 8.0 and were cleared by centrifugation and passage through a 0.45-μm filter. In each case the labeled IgG was eluted as a single peak from HPLC size exclusion chromatography and was used without further purification. Dilutions were made with the same buffer used in the dialysis, and the samples were injected through 0.45 μm filters into the light scattering cuvettes.

The protein concentrations were determined spectrophotometrically. Correction was made for the absorbance of the dye at 280 nm by means of the relation $(OD_{280})_{protein} = (OD_{280})_{total} - R(OD_{max})_{dye}$, where R is the ratio of the molar extinction coefficient of the dye at 280 nm to its maximum value. The R value of FITC at pH 8.0 is found to be 0.35, in agreement with Steinbach and Mayersbach.[6] The R value for ABITC was assumed to be the same as that for glycine-ABITC, which we determined to be 0.32. The extinction coefficient for IgG at 280 nm was taken to be 1.33 $L \cdot g^{-1} \cdot cm^{-1}$.[7]

C. Characterization of Labeled IgG. The average number of dye molecules per protein molecule was also estimated spectrophotometrically. We determined a molar extinction coefficient of 19000 $L \cdot mol^{-1} \cdot cm^{-1}$ at 355 nm for glycine-ABITC in 0.1 M NaCl, 0.05 M Tris at pH 8.0. Since the λ_{max} values for glycine-ABITC and IgG-ABITC were similar, their extinction coefficients were assumed to be equal. For IgG-FITC a molar extinction coefficient of 42500 $L \cdot mol^{-1} \cdot cm^{-1}$ at 495 nm has been reported by Tengerdy.[8] On the basis of these numbers we estimate the average number of dye molecules per protein molecule to be 2.4:1 for IgG-ABITC and 1.6:1 for IgG-FITC.

Classical, intensity vs. angle, light scattering was used to estimate the molecular weights of labeled IgG's. Measurements were made with a C. N. Wood Model 6000 light scattering monophotometer with a 5-mW He–Ne laser as the light source. Solutions of labeled and unlabeled IgG in buffer (0.1 M NaCl, 0.05 Tris, pH 8.0) were centrifuged at 37000g for 1 h prior to use. The solutions were then circulated through a 0.2-μm filter to minimize dust contamination. Zimm plots of the intensity measurements for unlabeled IgG and IgG-FITC yielded apparent molecular weights of approximately 150000 as expected for IgG monomers.[9] However, the intensity measurements for IgG-ABITC gave an apparent molecular weight much in excess of 150000, indicating the presence of aggregates. The degree of aggregation depends strongly on the pH used for the conjugation reaction, with high pHs favoring aggregation. With conjugation at pH 11.5, the apparent molecular weight turned out to be 435000.

D. HRS Experiment. The spectrometer and the methodology of HRS have been described in detail elsewhere.[2,10] A Spectra Physics 165 argon ion laser operating at 488 nm supplied the two beams which were used to write the grating. The fringe spacing in the grating was given by $\Lambda = \lambda/[2 \sin(\theta_w/2)]$, where λ is the laser wavelength and θ_w is the crossing angle of the beams, both measured in air. The duration of the writing laser pulse was approximately 2 ms and the average power was less than 80 mW. The reading laser beam was provided by a low-power He–Ne laser. Electromechanical shutters were used to define the duration of the writing laser exposure and to limit the on-time for the reading laser beam. The temperature of the sample cell was maintained at 20.0 ± 0.2 °C by means of a water-cooled cell holder.

The "phase shift and add" method was used to accumulate signals so that the cross-term between the diffracted signal and the coherent stray light could be eliminated.[11] The time-dependent signals (minus background) could be represented in all cases by

$$H_1(t) = a_1^2 \exp(-2\Gamma_1 t) + a_2^2 \exp(-2\Gamma_2 t) + 2a_1 a_2 \exp[-(\Gamma_1 + \Gamma_2)t] \cos(\phi_1 - \phi_2) \quad (1)$$

where $\Gamma_i = D_i K^2$, D_i is the diffusion coefficient of the ith species, K is 2π divided by the fringe spacing, and a_i and ϕ_i are the scattering amplitude and the relative phase angle of the ith species, respectively. The components of the experimental decay signals $H_1(t)$ were resolved by means of a nonlinear least-squares fitting program based on Marquardt's algorithm.[12] Then plots of Γ_i vs. K^2 were constructed in order to obtain values of D_i from the slopes and to investigate the intercepts. All of the plots had zero intercepts, which confirmed the absence of competing nondiffusive decay mechanisms. For the data reported here, decay curves were recorded and analyzed at least three times at two or more different values of K for each concentration of the protein.

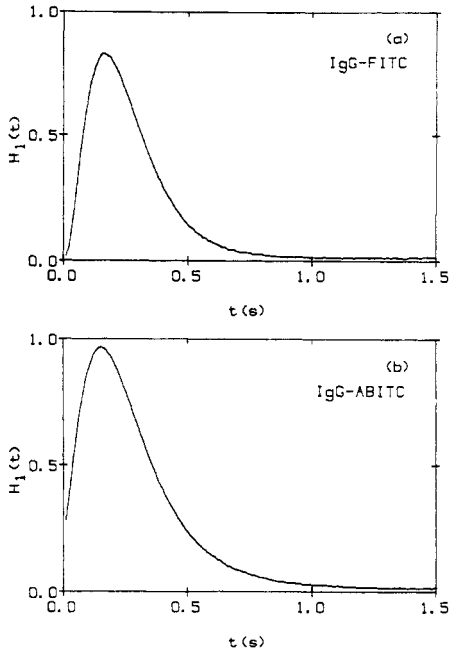

Figure 1. (a) A transient decay recorded with IgG-FITC in a "phase shift and add" experiment. (b) A transient decay recorded with IgG-ABITC in a "phase shift and add" experiment.

Results

A. HRS Analysis. Typical transient decay signals for IgG-FITC and IgG-ABITC are shown in Figure 1, parts a and b, respectively. As noted above, these curves are well described by eq 1. This indicates the presence of two diffraction species in each case, and we interpret the small signals at $t = 0$ as resulting from interference effects.[11] For IgG-FITC, where initial signal cancellation is complete, excitation of the label by the writing laser apparently creates a photoproduct which does not differ significantly in diffraction efficiency from the starting material. The best fit curve gives $a_1 = a_2$ and a phase difference of 180°. However, Figure 1b, which shows a nonzero minimum at $t = 0$ for IgG-ABITC, indicates a photoinduced change in the diffracting efficiency of the labeled molecule. The least-squares analyses for this label gave $a_1 < a_2$ and indicated that the phase difference was less than 180°. Here a_1 is associated with the faster component. A phase shift of 180° is, of course, expected between the concentration patterns of ground states and photoproducts since the ground state must be depleted at locations where photoreactions occur. The phase shift detected here, however, depends also on the relative magnitudes of the real and imaginary parts of the complex index of refraction grating associated with each species.[10]

Figure 2 shows the measured diffusion coefficients vs. total protein concentration for IgG-FITC and IgG-ABITC. Each analysis yielded two values of D, the larger one corresponding to the magnitude expected for monomer IgG.[13,14] The smaller values are approximately one-third the diffusion coefficient for a monomer and presumably indicate the presence of aggregates. At concentrations less than 20 g/L the decay curves for IgG-ABITC showed smaller contributions from the fast component, and the resolution into components was less accurate. On the basis of the results for IgG-FITC below 20 g/L and the results for IgG-ABITC at concentration greater than 20 g/L we conclude that the zero-concentration value of D for the fast component is $(4.5 \pm 0.5) \times 10^{-7}$ cm^2/s. The extrapolated value for the slow component from the IgG-ABITC data is $(1.9 \pm 0.1) \times 10^{-7}$ cm^2/s, while the IgG-FITC measurements give $(2.1 \pm 0.1) \times 10^{-7}$ cm^2/s.

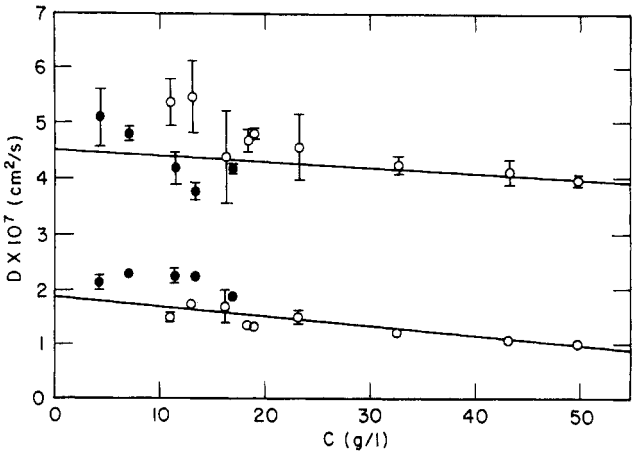

Figure 2. Diffusion coefficients for monomers and aggregates of IgG-FITC (●) and IgG-ABITC (○). Each pair of data points at the same concentration resulted from the resolution of an experimental decay curve (see text).

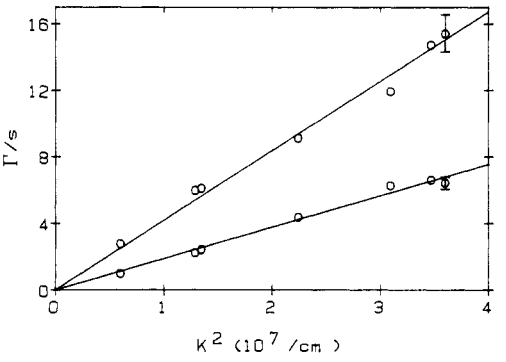

Figure 3. Decay constant Γ vs. K^2 for IgG-FITC at pH 8.0. The concentration was 19.8 g/L.

These results raise two questions. First, since a photochemical reaction is presumably involved which produces two sizes of particles through aggregation or disaggregation reactions, should not growth and decay of concentrations resulting from these reactions be considered in the analysis? Second, since the measured diffusion coefficients for the fast and slow components only differ by a factor between 2 and 3, can they really be resolved with such high accuracy? It is well-known that the decay constant for a diffusive process is proportional to K^2 while chemical reaction rates do not depend on K. Therefore, we have carried out an extensive series of experiments with different values of K in order to search for evidence of chemical reactions during the observation period. A typical plot of Γ vs. K_2 is shown in Figure 3 for IgG-FITC. As noted in the previous section, all such plots had zero intercepts and showed no evidence of nondiffusive contributions. Figure 3 also indicates the quality of our data. The error bars, which represent one standard deviation, were smaller than the symbols in the Figure 3 except where shown. The most meaningful indication of the errors is of course the scatter of the data points about the best fit line.

Apparently, the photoinduced reactions occur during the 2-ms pulse from the writing laser or shortly thereafter. In any event the diffraction efficiency during the first few seconds after the exciting pulse is controlled by mass diffusion. The accuracy of the separation of the two components results from the high signal-to-noise ratios and a favorable set of parameters. For example, in the case of IgG-FITC the two components have exactly the same

scattering efficiency and are out of phase by 180°. The only variable parameter is the ratio of the diffusion coefficients. It turns out that the shape of the curve in Figure 1a is fairly sensitive to this ratio.

B. Photobleaching Experiments. In order to investigate the effects of light on IgG-FITC and IgG-ABITC, and in particular to look for evidence of irreversible changes, we irradiated both materials for an hour with a 275-W sun lamp at 15 cm and with a 488-nm argon laser beam having an intensity of 50 mW/cm^2. In each case buffered samples at pH 8.0 were used, and the protein concentrations were approximately 4 g/L.

With IgG-FITC, irradiation caused absorption at the 495-nm maximum to decrease almost to zero. The 488-nm laser beam was especially effective in this transformation. The absorption did not recover after an hour in the dark, and we conclude that the change is irreversible. The absorbance at 280 nm was measured before and after irradiation, and no significant change was found. Therefore, the protein concentration was unaffected by irradiation and aggregation-induced precipitation was not a factor in the absorption change detected at 495 nm.

Irradiation of IgG-ABITC with either light source caused the absorbances at 360 and 450 nm to undergo a small increase and a small decrease, respectively. However, the absorbance values at both wavelengths were completely recovered after an hour in the dark. This is, of course, consistent with a reversible photoinduced trans–cis transition in the attached azobenzene moieties.

C. Inhibition of Oxygen-Related Aggregation. In order to confirm the photoinduced aggregation which was indicated by the HRS results for IgG-FITC, we attempted to inhibit the aggregation. It has been shown in some cases that irradiation of FITC-labeled proteins produces a build up of high molecular weight material.[15,16] It is known that photoexcitation of FITC produces a free radical,[16] and it has been suggested either that this free radical reacts directly with the protein or that it induces the formation of free singlet oxygen which in turn produces cross-linking. Therefore, cross-linking might be inhibited by quenching singlet oxygen, by removing oxygen altogether, or by reducing disulfide bonds.

These ideas were tested with a 0.1 mM solution of IgG-FITC, which initially gave strong HRS signals. First, the reducing agent glutathione or penicillamine was introduced. In each case 10 μL of 200 mM reducing solution was injected, resulting in the total disappearance of the HRS signals. In a separate experiment, HRS-active samples were purged with nitrogen and subjected to reduced pressure to remove free molecular oxygen. Again the HRS signals totally disappeared; however, the signal was partially restored upon reexposure to air. For comparison, similar experiments were performed with IgG-ABITC samples. In that case the HRS signals were only slightly reduced.

Discussion

The light scattering intensity measurements for IgG-FITC show that only monomers are present initially. However, the HRS experiments clearly demonstrate the presence of aggregates having diffusion coefficients only one-third that expected for monomers. Moreover, the HRS analysis indicates that the monomers and aggregates have similar optical properties to the extent that they diffract the 633-nm probe beam with the same efficiency. Finally, the HRS signals remain strong through many repetitions of the experiment, and there is little evidence of irreversible bleaching.

We interpret these findings as follows. Photoexcitation of FITC with the low-intensity short-duration pulse, which is used in HRS, does not cause irreversible bleaching.[17] It does, however, induce aggregation of IgG-FITC. Since the aggregation process is dependent on the presence of molecular oxygen and is inhibited by the reducing agents, it is likely that singlet oxygen is involved. The HRS signal from IgG-FITC is observed only because the monomers and aggregates have different diffusion rates. Otherwise, complete cancellation of diffracted light would occur at all times. In general FITC may not be a satisfactory label for use in HRS experiments since it does not provide a direct mechanism for the creation of an index of refraction grating, at least when visible radiation is used for excitation.

The experiments with IgG-ABITC are more consistent with our earlier studies of BSA-ABITC. Photoexcitation of IgG-ABITC does create an index of refraction grating and a nonzero signal immediately after the writing pulse. However, in the experiments reported here the sample of IgG-ABITC contained a significant fraction of aggregates prior to irradiation. The conjugation reaction, which is complicated by the insolubility of ABITC, proceeds more quickly at high pH, but the degree of aggregation also increases. The HRS analysis for IgG-ABITC shows two out-of-phase gratings as were found with IgG-FITC, but the interpretation is quite different. The results of the bleaching experiment and the insensitivity to oxygen and reducing agents are consistent with a photoinduced trans–cis conformational change for ABITC. The fact that complementary gratings of monomers and aggregates resulted from exposure to the writing laser indicates that the photoexcitation either induces additional aggregation or dissociates existing aggregates. At this time we favor the latter possibility. The cis form of ABITC is polar and its presence leads to enhanced solvation. This is consistent with our experiments and with the recently reported light-induced disaggregation of photochromic polypeptides.[18]

One final point must be made about the diffusion coefficients reported here. Since the laser-induced reactions produce new species or at least change the concentration of distinguishable species, this is not a tracer experiment. Real concentration gradients are present and the measured diffusion coefficients apparently refer to mutual diffusion. However, we have extrapolated the results to zero concentration, where mutual and tracer diffusion coefficients are equal.

Acknowledgment. This work was supported in part under National Science Foundation Grant CHE-8317243 to C.S.J. and National Institutes of Health Grant GM33865 and a Whitaker Foundation Grant to D.A.G.

References and Notes

(1) Hervet, H.; Urbach, W.; Rondelez, F. *J. Chem. Phys.* **1978**, *68*, 2725–2729.
(2) Miles, D. G.; Lamb, P. D.; Rhee, K. W.; Johnson, C. S., Jr. *J. Phys. Chem.* **1983**, *87*, 4815–4822.
(3) Arunyawongsakorn, U.; Johnson, C. S., Jr.; Gabriel, D. A. *Anal. Biochem.* **1985**, *146*, 265–270.
(4) Kaufman, G. I.; Nester, J. F.; Wasserman, D. E. *J. Histochem. Cytochem.* **1971**, *19*, 469–476.
(5) Coutandin, J.; Sillescu, H.; Voelkel, R. *Makromol. Chem., Rapid Commun.* **1982**, *3*, 649–652.
(6) Steinbach, G.; Mayersbach, H. V. *Acta Histochem. Bd.* **1976**, *55*, s.110–123.
(7) *Handbook of Biochemistry and Molecular Biology*, 3rd ed., "Proteins", Fasman, G. D., Ed; CRC Press: Cleveland, Ohio, 1975, Vol. II, 1975, p 452.
(8) Tengerdy, R. P.; Chang, C. A. *Anal. Biochem.* **1966**, *16*, 377–383.
(9) Gabriel, D. A.; Hadler, N. M. *J. Biol. Chem.* **1981**, *256*, 3240–3244.

(10) Rhee, K. W.; Gabriel, D. A.; Johnson, C. S., Jr. *J. Phys. Chem.* **1984**, *88*, 4010-4015.
(11) Johnson, C. S., Jr. *J. Opt. Soc. Am. B* **1985**, *2*, 317-321.
(12) Bevington, P. H. *Data Reduction and Error Analysis for the Physical Sciences*; McGraw-Hill: New York, 1969; Chapter 11.
(13) Hall, C. G.; Abramhan, G. N. *Arch. Biochem. Biophys.* **1984**, *233*, 330-337.
(14) Biserka, P.; Zvonimir, P. *Anal. Biochem.* **1979**, *93*, 103-114.
(15) Lepock, J. R.; Thompson, J. E.; Kruuv, J.; Wallach, D. F. H. *Biochem. Biophys. Res. Commun.* **1978**, *85*, 344-350.
(16) Sheetz, M. P.; Koppel, D. E. *Proc. Natl. Acad. Sci. U.S.A.* **1979**, *76*, 3314-3317.
(17) Schauenstein, K.; Wick, G.; Herzog, F.; Steinbatz, A. *J. Immunol. Methods* **1975**, *8*, 9-16.
(18) Pieroni, O.; Fissi, A.; Houben, J. L.; Ciardelli, F. *J. Am. Chem. Soc.* **1975**, *107*, 2990-2991.

Photopolymerization of Cyclohexene Oxide by the Use of Photodecomposable Silyl Peroxide. Aluminum Complex/Arylsilyl Peroxide Catalyst

Shuzi Hayase,* Yasunobu Onishi, Shuichi Suzuki, and Moriyasu Wada

Chemical Laboratory, Toshiba Corporation, Research and Development Center, Komukai Toshiba Cho, Saiwai Ku, Kawasaki 210, Japan. *Received August 13, 1985*

ABSTRACT: A new photoinitiating catalyst for epoxides was found. Catalysts that have been reported so far release strong inorganic acids, which this new catalyst does not produce. This new catalyst consists of an aluminum compound and triarylsilyl peroxide, some of which were newly synthesized. The reaction mechanism of this catalyst is proposed as follows: The arylsilyl peroxide was photodecomposed to form aryl silanol. Then the arylsilanol interacted with the aluminum compound and formed a cationic catalyst, which had been reported by the present authors. This composite catalyst initiated the polymerization of epoxides cationically. Epoxides did not polymerize in the absence of UV light. The arylsilyl peroxide was stable thermally below 150 °C. Quantum yields of the photodecomposition of various silyl peroxides were measured. The photogeneration of the arylsilanol was influenced by the wavelength, structure of arylsilyl peroxide, temperature, and solvent used. Photodecomposition products were analyzed, and the photodecomposition mechanism was proposed. The relationship between the structure of the silyl peroxide and the catalyst activity was also investigated. The catalyst having the highest activity was tris(ethyl 3-oxobutanoato)aluminum and tri-2-naphthylsilyl *tert*-butyl peroxide.

Introduction

Some photoinitiation catalysts for epoxide polymerization are known.[1-15] For example, diazonium salts of Lewis acids are well-known.[1-6] Recently, Crivello reported other new photoinitiation catalysts,[7-12] namely, sulfonium salts and iodonium salts of HBF_4, $HAsF_6$, HPF_6, and $HSbF_6$. Photoinitiation mechanisms of these catalysts and synthesis of sensitive sulfonium salts were also reported.[16-18] These catalysts photodecompose to form strong inorganic acids that polymerize epoxides cationically. Therefore, in this report, we call these catalysts "strong-acid catalyst".

The present authors already reported a new catalyst,[19] which is a "non-strong-acid catalyst". The catalyst consists of an aluminum compound and the photodecomposable organosilane, *o*-nitrobenzyl triarylsilyl ether (ONBSi). The photopolymerization mechanism has two steps. The first step was the photogeneration of silanol from the ONBSi. The second step was the polymerization of epoxides by the resultant catalyst, which consists of an aluminum compound and arylsilanol. The quantum yield when the silanol was photogenerated from the ONBSi was 0.21 using UV light (365 nm). In this type of catalyst, any organosilane can be used if the organosilane is photodecomposed to form organosilanol; however, it is necessary for the photodecomposable organosilane to be very stable at room temperature and be photodecomposed swiftly to form arylsilanol at a high ratio. We investigated the photodecomposition of silane in order to find a more photosensitive catalyst than ONBSi and discovered that "arylsilyl peroxide" photogenerated silanol more effectively and could be used for the coinitiators in the photopolymerization catalyst. In order to clarify the characteristics of the catalyst, several new arylsilyl peroxides were prepared, and the relation between the catalyst structure and the activity was examined.

In this paper, the profile of the new catalyst, the mechanism of photodecomposition, and the photopolymerization characteristics and mechanism are reported.

Experimental Section

Cyclohexene oxide was dried over CaH_2 and then distilled and stored under a nitrogen atmosphere. Tris(ethyl 3-oxobutanoato)aluminum ($Al(etaa)_3$) was synthesized by reacting triisopropoxyaluminum with ethyl acetoacetate.[20] Triphenylsilyl *tert*-butyl peroxide (3Ph-Bu), diphenylbis(*tert*-butylperoxy)silane (2Ph-2Bu) and triphenylsilyl cumyl peroxide (3Ph-Cu) were prepared by the method described in the literature.[21,22] 1-naphthyldiphenylsilyl *tert*-butyl peroxide (ANa2Ph-Bu), tris(4-chlorophenyl)silyl *tert*-butyl peroxide (3ClPh-Bu), tri-2-naphthylsilyl *tert*-butyl peroxide (3BNa-Bu), (2-methylphenyl)diphenylsilyl *tert*-butyl peroxide (MePh2Ph-Bu), and di-1-naphthylbis(*tert*-butylperoxy)silane (2ANa-2Bu) were newly prepared.

ANa2Ph-Bu was prepared as follows. All materials were distilled under N_2, and all experiments were carried out in N_2.

Method 1. 1-Naphthyldiphenylsilyl Chloride (ANa2Ph-Cl). 1-Naphthyl bromide (20.7 g) in 100 mL of dried tetrahydrofuran (THF) was added dropwise to 100 mL of dried THF in which 2.4 g of Magnesium was dispersed. After the addition was completed, the reaction mixture was stirred for 1 h at 50 °C. The reaction mixture was added to a solution of 25.3 g of diphenyldichlorosilane in 100 mL of THF and stirred for 2 h at 50 °C. Then, half the volume of THF was removed by boiling, and 300 mL of dibutyl ether was added in order to precipitate the salt. The mixture was heated gradually to 100 °C in order to remove THF completely. After the precipitate was removed off,

0024-9297/86/2219-0968$01.50/0